

The Superconducting Levitated Dipole Experiment (LDX)

D.T. Garnier^{a,*}, A.K. Hansen^a, J. Kesner^b, M.E. Mauel^a,
P.C. Michael^b, J.V. Minervini^b, A. Radovinsky^b,
A. Zhukovsky^b, A. Boxer^b, J. Ellsworth^b, I. Karim^b, E. Ortiz^a

^a*Dept. Applied Physics and Applied Mathematics, Columbia University, 500 W.
120th St., New York, NY 10027 U.S.A.*

^b*Plasma Science and Fusion Center, Massachusetts Institute of Technology, 77
Massachusetts Ave., Cambridge, MA 02139 U.S.A.*

Abstract

The Levitated Dipole Experiment (LDX) explores the physics of high-temperature plasmas confined by a dipole magnetic field. Stable high-beta plasma has been created and confined by the magnetic field of a superconducting coil. Discharges containing trapped electrons form when microwaves cause strong perpendicular heating at cyclotron resonance. To eliminate the losses to the supports, the magnetic dipole (a superconducting solenoid) will be magnetically levitated for several hours. The dipole magnetic field is generated by a Nb₃Sn floating Coil (F-coil), a maximum field of 5.3 T, operating for up to 2 hours. A NbTi charging coil (C-coil) surrounds a portion of the vacuum chamber and induces the current in the floating coil. After the F-coil is lifted to the center of the chamber, the Levitation Coil (L-coil), made from high temperature superconductor, magnetically supports it. In the first year of operation, the device has been operated in a supported mode of operation while experience has been gained in the cryogenic performance of the F-coil and the integration of the F-coil and C-coil. Current work focuses on the integration of the F and L coils in preparation for first levitation tests.

Key words: Plasma confinement, Fusion engineering, Superconducting magnets
PACS: 52.55.-s, 52.50.SW, 52.35.-g

* Corresponding author. Tel.: +1-617-258-8997 Fax: +1-617-253-0448
Email address: garnier@psfc.mit.edu (D.T. Garnier).

¹ This research is supported by U.S. Department of Energy under Grants No. DE-FG02-98ER-54458 and DE-FG02-98ER-54459.

1 Introduction

The levitated dipole experiment (LDX) is a new research facility that was designed to investigate the confinement and stability of plasma in a dipole magnetic field configuration [1]. The dipole confinement concept was motivated by spacecraft observations of planetary magnetospheres that show centrally-peaked plasma pressure profiles forming naturally when the solar wind drives plasma circulation and heating [2]. Unlike most other approaches to magnetic confinement in which stability requires average good curvature and magnetic shear, MHD stability in a dipole derives from plasma compressibility [3–5]. Plasma is stable to interchange and ballooning instabilities when the pressure gradient is sufficiently gentle even when the local plasma pressure p exceeds the magnetic pressure $B^2/2\mu_0$ or, equivalently, when $\beta \equiv 2\mu_0 p/B^2 > 1$ [6].

Plasma physics experiments have been performed with the superconducting dipole supported by thin rods. These experiments demonstrated the production of high beta plasma confined by a laboratory dipole using neutral gas fueling and electron cyclotron resonance heating (ECRH) [7, 8]. The pressure results from a population of energetic trapped electrons that can be maintained for many seconds of microwave heating provided sufficient neutral gas is supplied to the plasma.

The LDX experiment is pictured in Fig. 1. LDX consists of a relatively small, 0.68 m diameter (current centroid), superconducting ring levitated within a 5 m diameter vacuum vessel. The absence of toroidal and vertical fields makes LDX considerably simpler than the levitron devices that were successfully operated several decades ago [9–12]. The magnet configuration, shown in Fig. 1, achieves levitation of the dipole using a high temperature superconducting magnet located at the top of the large vacuum chamber. The dipole’s position is stable to tilt and horizontal displacements and, as a result, only requires feedback control for the ring’s vertical position.

Studies by Hasegawa, *et al.* [13, 14] and by Teller, *et al.* [15] considered the application of a levitated dipole as a D-³He based power source. Advanced fuel cycles (D-³He, D-D) eliminate the need for tritium breeding and can significantly reduce 14 MeV neutron production and the associated structural damage. By incorporating an internal refrigerator in the floating ring a levitated dipole device would be intrinsically steady state. Such a device would deposit power on the first wall as surface heating, permitting a thin walled vacuum vessel and eliminating the need for a massive neutron shield. Since the confining magnetic field is produced by a coil that is internal to the plasma, the magnetic field decays as the plasma pressure falls off leading to a good utilization of the field. Therefore, although the vacuum chamber envisioned is relatively large, this does not lead to an unreasonably high magnetic field

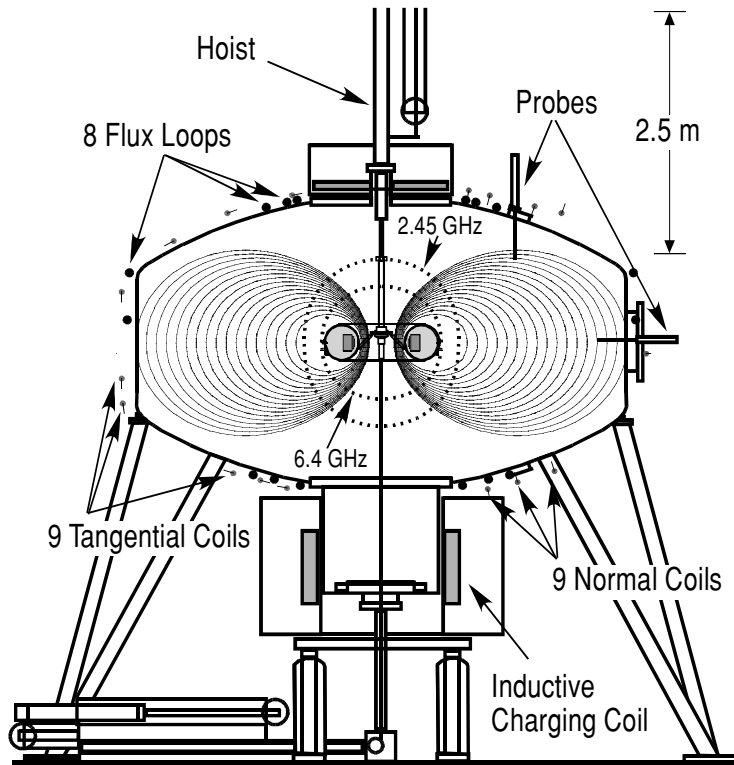


Fig. 1. Schematic of LDX experiment showing the dipole magnet suspended within the vacuum vessel. Loops and coils measure the equilibrium plasma current, and probes measure fluctuating potentials. Injected microwave power strongly heats electrons at the cyclotron resonance.

energy. There are no interlocking coils so that coil replacement, if necessary, could be relatively straight forward.

The D-D cycle is particularly interesting since the only fuel required is the plentiful deuterium. We have recently considered a dipole based system as a fusion power source [16] utilizing a fuel cycle which we call the “Helium catalyzed D-D” cycle in which the secondary ^3He is burned and the secondary tritium is recovered and reintroduced and burned much later as ^3He . In this design study, representative power system configurations were presented, and three-dimensional neutronics calculations were performed in order to estimate the heating rates and temperatures that would occur within the floating coil. Although Nevins [17] found that a D-D cycle is precluded in a tokamak because of the accumulation of fusion products, in a dipole the combination of high beta and high energy confinement with reduced particle confinement would make it ideally suited as a D-D based power source.

1.1 Physics Requirements

The sustainment of a dipole field using a coil that floats without supports for up to 2 hours requires a high performance superconducting coil encapsulated within a cryostat. The requirements for creating a fusion grade plasma using electron cyclotron heating (ECH) determined the size of the floating coil and the vacuum chamber as well as the choice of superconductor.

Since MHD interchange stability imposes a limitation on the pressure gradient in terms of magnetic flux tube differential volume ($U \equiv \oint dl/B$), an important design goal of LDX was to maximize the expansion of magnetic flux volume. This requires a relatively small coil to float within a large vacuum chamber. From MHD $p_0/p_{sol} < U_{sol}/U_0$ where a zero subscript designates core values and a “sol” subscript the edge. For the dipole, this ratio can be made very large, i.e. $p_0/p_{sol} > 10^3$.

In order to achieve high compressibility in the design of LDX, the strength of the magnetic field from the levitation coil had to be relatively small. The levitation coil supports the weight of the floating coil and the required radial field is $B_r = M_d g / 2\pi a I_d$, proportional to the ratio of the dipole’s weight, $M_d g$, to the dipole current, I_d where a is the average diameter of the coil. As a consequence, the superconduction dipole (F-coil) had to be designed so that the ratio of current to mass could be maximized. Furthermore, the use of electron cyclotron resonance heating at fusion relevant densities sets a requirement on the magnetic field level. We require that the 6.4 GHz heating frequency (resonant at $B = 0.23$ T) source of the planned multiple frequency heating system be resonant on the outer plasma midplane and on a field line that encloses the floating coil.

2 Facility Design

LDX requires the levitation of a relatively small coil within a large vacuum chamber. The large distance between the floating coil and the vessel and control magnets represented a design challenge. LDX, however, does not require strong toroidal and vertical fields and this greatly simplifies the stability and control of the LDX floating coil. Our base case magnet configuration, shown in Fig. 1, achieves ring levitation using a single, high temperature superconducting magnet located ~ 1.57 m above the floating coil. This configuration is stable to tilt and horizontal displacements and, as a result, LDX only requires feedback control to stabilize a slow ($\gamma \sim 4$ s⁻¹) instability in floating coil’s vertical position. This upper levitation was chosen because levitation by pushing from below is unstable to horizontal and tilting motions which

would require non-axisymmetric control coils and thus impact negatively on the plasma confinement. LDX uses a pneumatic “launcher” to mechanically lift the floating coil from the bottom of the vacuum vessel (from the so-called “charging station”) to the center of the vacuum vessel. At this location, the coil’s weight is counterbalanced by the levitation coil located at the top of the vacuum vessel. In effect, the floating coil hangs like a pendulum.

Careful design of the floating coil’s cryostat and a method to induce the coil’s very large operating current (> 1.2 MA) was necessary. The floating coil’s cryostat borrows some of the ideas used in the superconducting FM-1 ring previously built at PPPL [10, 11]. The method we’ve selected to charge the floating coil’s large current is induction. As a consequence, there are no high-current electrical contacts that need to be made and broken in the floating coil.

2.1 Superconducting Dipole Coil

The 550 kg floating coil (F-coil) is an inductively charged, superconducting magnet comprised of a single 1.5 km length conductor carrying over 1.5 MA turns in a persistent mode. The design of this conductor, coil and its cryostat was based on many of the advances in superconducting magnet technology made over the past 25 years and now widely used in large numbers of commercial MRI, NMR, accelerator and other high field magnet systems in reliable, long term operating service worldwide.

The F-coil conductor is based on a pre-reacted 18 strand Rutherford cable Nb₃Sn superconductor [18]. The advanced Nb₃Sn strand, a successor to the ITER EDA strand development, has a diameter of 0.75 mm and a relatively low copper fraction of 0.3. This design maximizes the current-sharing temperature at a given current, and therefore the experimental run time. The strand was then formed into a cable and heat treated to become a superconductor. The reacted cable was soldered into a half-hard 8 mm \times 2 mm copper channel for structural support and quench current sharing. The choice of reduced strand copper content with a hardened copper channel allows maximal superconductor performance at minimum coil weight, reducing the requirements on the external levitation coils and maximizing plasma volume.

The single 1.5 km long reacted cable was then insulated and wound in a hybrid single pancake/double layer fashion to form a continuous winding pack (716 turns) without internal joints and a persistent joint at the coil outer radius. The geometry of the winding pack is of three rectangular sub-coils with aligned vertical centers. The inner sub-coil has inner diameter of 0.552 m and height of 0.069 m; the next has inner diameter of 0.555 m and height

of 0.125 m, while the outer sub-coil has an inner diameter of 0.585 m, outer diameter of 0.764, and height of 0.162 m. The winding pack is free standing with all thermal and magnetic stresses internally maintained. The combination of internal conductor stabilization and nominally steady state operation should minimize unexpected quenching of the magnet. In the event of a quench, however, the coil is designed with passive quench protection to ensure hot spot propagation allowing the magnetic stored energy to be safely dumped within the winding pack thermal mass. The winding pack was epoxy vacuum-pressure impregnated and cured to provide structural integrity. After testing to full current in a liquid helium bath using current leads, a joint was made on the outer diameter of the coil so as to form a closed loop [19].

The cryostat [20] consists of a toroidal shaped inconel helium pressure vessel surrounded by a 316L stainless steel vacuum vessel (inner diameter 0.445 m, outer limiter diameter 1.14 m). Run time is maximized using a 60 kg inner lead radiation shield that provides additional inertial cooling at intermediate cryogenic temperature. The inconel pressure vessel is pressurized at room temperature to 125 atm and contains roughly 1.5 kg of helium gas cryogen. Over the operating temperature of the Nb₃Sn magnet from 4.3 to about 10 K, this small amount of helium provides the bulk of the thermal capacity of the 400 kg winding pack/inconel vessel cold mass. Utilizing a low heat leak cryostat design, the total heat leak to the cold mass is kept small, allowing an expected 2 hour levitation time.

The cryostat is cooled by a heat exchanger wrapped within the helium pressure vessel and then continues in series with a cooling tube embedded within the lead shield laminate. Liquid helium flows through the heat exchanger through a pair of bayonets that penetrate through the bottom of the charging station. The cryostat support system is built from 24 columns of powdered metal laminations designed to withstand up to 10 g overloading (in case of a loss of control event). The supports provide a very low heat leak at the normal operating conditions of the magnet.

In operation, the F-coil is cooled from the room temperature to 200 K by cold nitrogen gas then by liquid nitrogen to 80 K in about 76 hours. Cooling from 80 K to 4.4 K occurs in 5-6 hours using about 140 l of liquid helium (including cooling during F-coil charging). Re-cooling of the F-coil between experimental runs requires 40-50 minutes and consumes about 40 liters.

2.2 Charging Coil

The charging coil is used to charge the F-coil inductively to its operational current of 1820 A. The coil was designed by the Efremov Institute and MIT [21],

Table 1
CHARGING COIL PARAMETERS

Parameter	Units	Value
Layers		48
Turns		8388.5
Max. Operating Current	A	425
Stored energy	MJ	8.3
Peak field in windings	T	3.9
C-coil inductance - L_C	H	91.6
F-coil self inductance - L_F	H	0.389
Mutual inductance - M_{CF}	H	1.69

and was manufactured by the Efremov Institute. The coil is a solenoid wound with NbTi conductor and operates in a pool-boiling liquid helium cryostat, that surrounds the 1.157 m diameter charging station.

The conductor and C-coil winding pack were designed to satisfy the requirement that the maximum hot spot temperature after a quench be below 150 K, and the maximum voltage developed during a C-coil quench not exceed 3 kV. The conductor is a solder-impregnated compacted cable containing three superconducting strands co-twisted with seven copper wires. The coil was layer wound with the layer-to-layer joints located outside of the outer cylindrical surface of the coil. A mandrel-free vacuum-pressure impregnated self-supporting winding was utilized. The winding pack was designed with a height of 750 mm, and inner and outer diameters of 1300 and 1600 mm. The operating current of the C-coil is 425 A as shown in Table 1.

2.2.1 C-coil Cryostat

The C-coil is fixed within a mushroom-shaped helium vessel. An 80 K thermal shield which consists of an outer and an inner stainless steel liquid nitrogen vessels was located around the helium vessel. A vacuum can surrounds the thermal shield. The C-coil cryostat utilizes gas-cooled copper current leads. Cryogenic adsorption panels with a charcoal adsorbent have been installed on the liquid nitrogen vessel to maintain 10^{-7} torr operating vacuum in the cryostat.

In operation, the C-coil is cooled to 77 K with liquid nitrogen over a 75 hour period. The coil is then cooled to 4.2 K and the helium vessel filled with liquid helium over 30 hours. Consumption of liquid helium is about 1500 liters, including about 510 liters collected in the helium vessel. The operational

volume of liquid was about 170 liters above the magnet. The average boil off at the C-coil operation level is about 7.8 l/h, which corresponds to 5.5 W of the heat load. These figures include one-two charges/discharges up to 300 A. The operation time between necessary re-fills of the C-coil helium vessel is more than 12 hours.

2.2.2 C-coil Quench Protection System

A quench protection system (QPS) serves to protect the superconducting C-coil and the power supply in case of quench or a power supply failure. A four-quadrant 40 V and 600 A power supply is used for the charge/discharge of the C-coil. During the time when the F-coil is out of the charging station, the C-coil charging circuit must be open. To protect the C-coil from damage during a quench, the QPS must provide a fast discharge through a 5.7 Ω dump resistor leading to the maximum terminal voltage of the C-coil of 3 kV. The QPS is connected to the C-coil by high voltage cables and it will start to operate within 100 ms after a signal is received from the quench detection system.

When the QPS activates, a main thyristor electronic switch and a backup mechanical switch, which normally shorts out the dump resistor, receive the signal to open. At the same time, a crowbar is fired to add secondary protection to the C-coil power supply.

The detection system monitors the resistive voltage in the magnet and generates a signal for the QPS if the voltage reaches a threshold value of 50 mV. The F-coil has a significant effect in determining the quench condition. The C-coil has 6 voltage taps which permit the determination of the voltage across 4 coil segments. For segment i :

$$V_i = \left(L_i + \sum_j M_{ij} \right) \frac{dI_c}{dt} + R_i I_c + M_{if} \frac{dI_f}{dt} \quad (1)$$

where M_{ij} (M_{if}) is the mutual inductance between the C-coil segment i and segment j (or the floating coil, f). In the absence of the F-coil, i.e. for $I_f = 0$, a quench of the C-coil is readily detected by the appearance of a non-inductive resistance, R_i . To protect the magnet, we require the QPS to be triggered when this resistive voltage exceeds 50 mV.

As is typically done to detect quenches, bridge circuits are built between different segments of the coil to null out the contribution proportional to dI_c/dt . However, because the F-coil resistance changes during a C-coil charge cycle, a simple bridge circuit cannot be used. When the F-coil is superconducting, the bridge circuit response to the changing F-coil current is observed to give

voltages of ~ 150 mV. Thus, in order to maintain the required sensitivity, the bridge voltages are combined so as to cancel the F-coil response (proportional to dI_f/dt). Eddy currents can also be driven in other parts of the system, and they would show up as secondary coils in Eq. 1. However, it is unlikely that they are a significant effect as their decay times must be short compared to the voltage ramp time of the system ($L/R > 10$ s). Using an ad-hoc combination of four bridge circuit voltages, we are able to null out the system response to changes in the F-coil current and eddy currents to less than 20 mV.

2.3 Facility Operation

The F-coil is serviced and remains within the charging station except during times of plasma operation. The bottom of the charging station has flanges for plasma diagnostics, feeds for the F-coil, and a central flange for the launcher. The inlet and outlet transfer lines and the instrument connector can be engaged into the corresponding F-coil ports. The bottom of the F-coil is also equipped with an extra pump-out port with a plug, which can be removed by a plug operator attached to the bottom of the charging station. Opening this port permits the pumping of the F-coil by the large LDX vacuum pumping system. To insure that connecting-disconnecting the retractable cryogenic transfer lines with the F-coil ports does not spoil the high vacuum in the LDX plasma chamber ($10^{-6} - 10^{-8}$ Torr), guard tubes engage the F-coil ports and hermetically seal the space around the transfer lines from the surrounding vacuum in the charging station. Removable plugs are also placed in the heat exchanger ports, though the guard tubes, to seal the F-coil heat exchanger from plasma fill gases.

The sequence of LDX operation [22–24] is as follows: The C-coil is charged in about 25 minutes to the maximum current (425 A), when the F-coil is still in the normal state (above 17 K), which corresponds to the helium vessel temperature above 20 K. When the temperature drops below 8 K the C-coil is discharged inducing the full current to the F-coil. After the helium vessel reaches 4.5 K it is cooled further for 20-30 minutes. When the helium vessel reaches the minimum temperature of about 4.3 K the LHe flow is terminated. Next, the transfer lines are retracted, the heat exchanger is pumped, and its ports are plugged. The instrument connector is then detached and the vacuum guard tubes are retracted from the F-coil ports. The C-coil is open circuited to ensure zero current is induced, and thus zero force, as the F-coil is lifted out of the charging station and during LDX plasma experiments. After ~ 2 hours the F-coil is lowered back to the charging station and is rotated on a centering rotary ring into the correct position such that the guard tubes and the instrument connector can be engaged into the cryostat ports. If the helium vessel temperature is below 10 K, the F-coil can be re-cooled by LHe

flow through the transfer lines. Otherwise, the C-coil can be ramped up (the main charging circuit is closed) to discharge the F-coil. An F-coil quench will occur when the He vessel reaches 13.5K. At the end of the experimental period the F-coil is warmed up by a He flow to above 20 K, so that the C-coil can be safely discharged.

2.4 Levitation Coil

The LDX experiment achieves levitation of the 550 kg floating coil, by means of a disk-shaped, high-temperature superconducting levitation coil (the L-Coil), that is mounted on top of the vacuum vessel [25,26]. The main benefits of using a high temperature superconducting coil are greatly reduced electric power and cooling requirements. The L-Coil will be operated at 0.9 T and 20 K. The coil is helium-free being conduction cooled with 20 K, 20 W single stage cryocooler and surrounded by a LN2 shield. It has a protection circuit that not only protects it against overheating in the event of quench, but also against a F-Coil collision in the event of a control failure.

The high-temperature superconductor to be used in the L-Coil is a 0.17 mm \times 3.1 mm commercially-available BSSCO-2223 tape, supplied by the American Superconductor Corporation (AMSC). It is close to being state-of-the-art in terms of having the best combination of critical properties and strength for the application. It is characterized by a critical current of 62 A at 77 K and self-field. The tape properties are described in Table 2.

The Levitation Coil (L-Coil) is a disk-shaped magnet, consisting of a double pancake winding, 34 internal joints, and terminations at the outer radius. The pancakes are wound to either side of a center support plate which consists of two 1.0 mm thick copper sheets that are epoxy laminated to either side a 9.5 mm thick stainless steel plate. The copper sheets, which have several thin radial electric breaks to minimize eddy currents, are used for thermal conduction cooling from a single-stage cryocooler cold head. The main parameters of the L-Coil winding pack are given in Table 2.

2.5 Levitation Control System

The levitation control system is primarily comprised of coil position sensing system and a fast digital feedback system to control the L-coil power supply. Other components include a slow process logic controller to monitor the L-coil and provide quench detection and a backup position detector to provide a failsafe against an upward loss of control event.

Table 2
L-COIL WINDING PACK PARAMETERS

Parameter	Units	Value
tape width	(mm)	3.1 ± 0.2
tape height	(mm)	0.168 ± 0.02
I_c (20 K, 0 T)	(A)	≈ 175
I_{op}	(A)	125
Inner Diameter	(mm)	410
Outer Diameter	(mm)	1320
# turns		2800
Length BSSCO tape	(km)	7.3
Stored energy	(kJ)	20.4
$V_{crowbar}$	(V)	280
L-F vertical separation	(m)	1.566

Five degrees of freedom of the floating coil, its position in space and its two tilt axes, are diagnosed by a set of 8 lasers that are occulted by a cylindrical ring mounted on the outer shell of the F-coil. These commercially available lasers sensors (Keyence Corp. Model LV-H300) have 3 cm wide ribbon shaped beams that when blocked give a sensor signal proportional to the amount of occultation. Thus, using two lasers oriented in the horizontal Y direction, passing on either side of the F-coil ring, we obtain (redundantly) a measure of the X position with $10 \mu\text{m}$ accuracy. Using 4 vertically oriented sensors we also obtain the vertical position and tilts with redundancy. Determination of the rotation of the floating coil is made by observing reflected light from stripes made on the surface of the detection ring.

The digital control system is comprised of a computer with multiple channels of digital and analog input and output. Using a digital system allows for a more flexible implementation of the control algorithm. Using a realtime operating system (QNX Neutrino) ensures that the feedback cycle runs deterministically with high reliability, driven from a hardware clock at 5 kHz. Although the fastest modes of the levitated system (the tilt oscillation) is less than 10 Hz, this faster feedback cycle allows for more filtering and thus better noise isolation. The feedback algorithm is implemented using RT-Lab from Opal-RT and programmed using Mathworks Simulink which also allows the dynamical system to be simulated. The feedback algorithm will be optimized to minimize the AC loss heating of the L-coil based on the measured noise in the system during the test phase.

2.6 Shaping Coils

In addition to the main superconducting coils in LDX, there is a copper Helmholtz coil set that allows the volume of the plasma, and thus the compressibility, to be changed significantly. The Helmholtz coils have a radius of 2.44m and are composed of 16 turns of copper wire, capable of carrying up to 2000 A.

3 Experiments with a Supported Internal Coil

The time evolution of plasma discharges created in LDX shows the plasma to exist within one of three plasma regimes: the “low density” regime early in the shot (typically $0 < t < 0.3$ s), the “high beta” regime that follows a transition, and the “afterglow” that occurs after the ECRH power is switched off. Figure 2 shows diagnostic signals from a typical LDX high-beta discharge, in which 5 kW of total ECRH microwave power was applied to the plasma with equal amounts from 2.45 GHz and 6.4 GHz sources. The deuterium pressure was adjusted with four pre-programmed gas puffs. After an initial period typically lasting 0.25 s, the plasma is observed to enter a high beta phase. When the ECRH power is switched-off, the plasma equilibrium current slowly decays proportional to the collisional loss rate of the trapped electrons.

In the low density regime, the plasma is characterized by relatively small diamagnetism (~ 0.1 mV·s) and line-density ($\sim 2.3 \times 10^{16}$ m⁻³) and exhibits evidence of rapid radial transport. A significant x-ray signal is observed on a NaI detector with a radial view that includes the floating-coil, which we know indicates inward-moving hot electrons striking the surface of the dipole coil. Negatively biased Langmuir probes at the outer edge of the plasma measure intense bursts of outward-directed energetic electrons. High-speed recordings of the electrostatic potential fluctuations show frequencies that resonate with the magnetic drifts of electrons with energies ranging from 20-60 keV. As observed previously in a supported dipole experiment, [28–30] the hot electron interchange (HEI) instability appears as quasi-periodic bursts with frequencies that are $\approx 0.3\omega_{dh}$, where ω_{dh} is the hot electron diamagnetic drift frequency, and sweep to higher frequencies, $\omega \sim 1.8\omega_{dh}$, during the nonlinear saturation of the instability.

The high-beta regime occurs after an abrupt transition that occurs when the neutral gas pressure exceeds a critical level that ranges from $2.5\text{--}3.5 \times 10^{-6}$ Torr. The level of neutral gas pressure required for the transition increases with the level of microwave heating power and varies when the outer shape of the plasma is modified. Typically the transition occurs rapidly, within 2 ms,

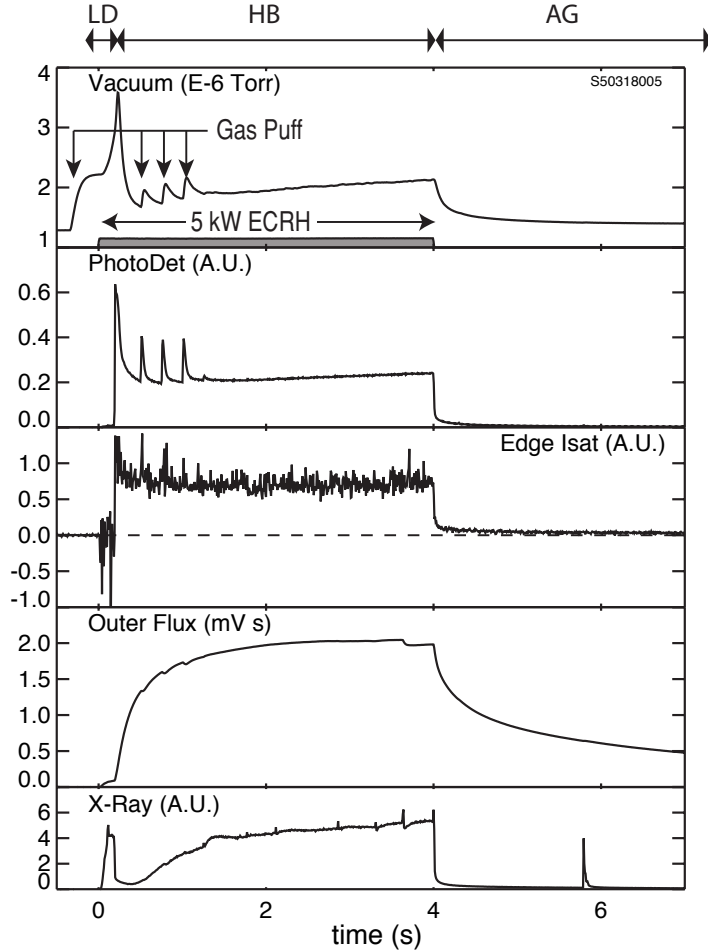


Fig. 2. Example high beta plasma discharge created with 5 kW ECRH power and four gas puffs. Measurements show (i) the deuterium gas pressure within the chamber, (ii) the visible light from the plasma, (iii) the ion saturation current near the plasma edge, (iv) the magnetic flux near the outer equator, and (v) the x-ray intensity.

and coincides with the ionization of the background neutrals and a rapid buildup of plasma density to a value 7-10 times larger than during the low-density regime. A 10-20 fold buildup of plasma diamagnetism occurs over a much longer interval, ~ 0.5 s. Initially, as the density rises, the detected x-ray intensity decreases by an order of magnitude consistent with the elimination of inward hot electron flux to the floating coil. The sign of the current collected by the negatively-biased edge probes reverses, so that positive ion saturation current is collected, indicating a sharp decrease in radial transport of fast electrons. Hard x-ray images indicates a hot electron anisotropy of $p_{\perp}/p_{\parallel} \sim 5$. High-speed floating potential probe measurements show the HEI instability is stable after the transition to the high-beta regime.

When the microwave power is switched off, the plasma evolves to the regime called the “afterglow”. The plasma density decays within 10-15 ms, while the

energetic trapped electron population decays much more slowly (1-20 s) consistent with the pitch angle scattering rate of hot electrons. The slow decay of the diamagnetism indicates that the bulk of the stored energy is contained in the hot electron population while the fast decay of plasma density indicates that a significant fraction of the injected microwave power is required to maintain the density of the cooler plasma.

Estimates of the plasma pressure are made by computing the least-squares best-fit of a model to the magnetic diagnostics assuming an anisotropic pressure profile. Plasma with the highest values of I_p and β are created with both 2.45 GHz and 6.4 GHz heating. The sum of the mean-square deviations between the best-fit model profile and the magnetic measurements doubles as compared with single-frequency heating, and this may be related to the presence of two pressure peaks, one at each resonance. If R_{peak} is assumed to be midway between the resonances and $p_{\perp}/p_{\parallel} = 5$, then 5 kW of heating creates a plasma (discharge No. 50513029) with $I_p = 3.5$ kA, $\Delta I_f = -0.8$ kA, $W_p = 330$ J, $p_{\perp} = 750$ Pa, and maximum local beta of $\beta = (2\beta_{\perp} + \beta_{\parallel})/321\%$. If R_{peak} moves outward closer to the 2.45 GHz resonance by 5 cm, $\beta = 23\%$; moving inward by 4 cm towards the 6.4 GHz resonance, the best-fit results in $\beta = 18\%$.

4 Conclusions

The LDX experiment began operation in August 2004. Using multi-frequency electron cyclotron resonance heating (ECRH), high-beta plasmas have been created, sustained for many seconds, and studied while the high-field dipole magnet was mechanically-supported by three, thin (1 cm dia.) support rods. These experiments were the first stage of a carefully planned operational program that allows for the safe and reliable operation of the three LDX superconducting magnets and the coordinated installation and test of diagnostics and research tools. During our first stage operation, significant programmatic and scientific results were achieved including: (i) demonstration of reliable operation of the high-field superconducting magnets, (ii) long-pulse, quasi-steady-state (> 10 s) plasma formation using ECRH, (iii) achievement of peak equatorial plasma beta near 20%, (iv) operation of all base diagnostics and data acquisition systems, (v) identification and parameterization of three discharge “regimes” having unique physics properties, (vi) preliminary study of ECRH profile control using multiple-frequency heating, (vii) identification of beta-limiting instability driven by a large fractional density of energetic trapped electrons, (viii) preliminary study of plasma shape effects, (ix) preliminary study of plasma density profile using movable edge probes and a single-cord microwave interferometer, and (x) preliminary study of x-ray emissivity using an array of x-ray detectors. These first-stage experiments, using a supported

dipole, are nearly complete. Future experiments are planned in which the coil will be levitated.

Acknowledgment

We gratefully acknowledge the technical expertise of J. Schultz, B. Smith, V. Fishman, R. Latons, D. Strahan and S. Zweben.

References

- [1] J. Kesner, L. Bromberg, D.T. Garnier, M.E. Mauel, in *Fusion Energy 1998* (IAEA, Vienna, 1999) Vol. 3, p 1165.
- [2] A. Hasegawa, Comments Plasma Phys. Controlled Fusion, **1**, (1987) 147.
- [3] M.N. Rosenbluth and C.L. Longmire, Ann. Phys. **1**, (1957) 120.
- [4] I.B. Bernstein, E. Frieman, M. Kruskal, R. Kulsrud, Proc. R. Soc. Lond. A **244** (1958) 17.
- [5] T. Gold, J. Geophys. Res., **64** (1959) 123.
- [6] D.T. Garnier, J. Kesner, M.E. Mauel, Phys. Plasmas **6**, (1999) 3431.
- [7] D. T. Garnier, A. Boxer, J. Ellsworth, A. Hansen, I. Karim, J. Kesner, S. Mahar, M. E. Mauel, E. Ortiz, A. Roach, “Stable High Beta Plasmas Confined by a Dipole Magnetic Field”, Submitted to Physical Review Letters, (2005).
- [8] D. T. Garnier, A. Boxer, J. Ellsworth, A. Hansen, I. Karim, J. Kesner, S. Mahar, M. E. Mauel, E. Ortiz, A. Roach, “Production and Study of High-Beta Plasma Confined by a Superconducting Dipole Magnet”, Submitted to Physics of Plasmas, (2005).
- [9] G. Navratil, R.S. Post and A. Butcher Ehrhardt, Phys Fluids **20**, (1977) 157.
- [10] R. Freeman, *et al.*, “Confinement of plasmas in the spherator”, in *Plasma Physics and Controlled Nuclear Fusion Research* (IAEA, Vienna, 1972) Vol. 1, 27.
- [11] O .A. Anderson, *et al.*, in *Plasma Physics and Controlled Nuclear Fusion* (IAEA, Vienna, 1972) Vol. 1, 103.
- [12] M. Okabayashi, *et al.*, Phys. Fluids **16** (1973) 1337.
- [13] A. Hasegawa, L. Chen and M. Mauel, Nuclear Fus. **30**, (1990) 2405.
- [14] A. Hasegawa, L. Chen, M. Mauel, H. Warren, S. Murakami, Fusion Technology **22** (1992) 27.

- [15] E. Teller, A. Glass, T.K. Fowler et al., *Fusion Technology* **22**, (1992) 82.
- [16] J. Kesner, D.T. Garnier, A. Hansen, M. Mauel, L. Bromberg, *Nucl. Fusion* **44** (2004) 193.
- [17] W.M. Nevins, *Journal of Fusion Energy* **17**, (1998) 25.
- [18] B.A. Smith, J.H. Schultz, A. Zhukovsky, A. Radovinsky, C. Gung, P.C. Michael, *et al.*, “Design, Fabrication and Test of the React and Wind, Nb₃Sn, LDX Floating Coil”, *IEEE Trans. Appl. Supercond.*, **11** (2001) 2010.
- [19] A. Zhukovsky, D. Garnier, C. Gung, J. Kesner, M. Mauel, P. Michael, *et al.*, *IEEE Trans. Appl. Supercond.*, **12** (2002) 666.
- [20] A. Zhukovsky, M. Morgan, D. Garnier, A. Radovinsky, B. Smith, J. Schultz, *et al.*, “Design and Fabrication of the Cryostat for the Floating Coil of the Levitated Dipole Experiment (LDX)”, *IEEE Trans. Appl. Supercond.*, **10** (2000) 1522.
- [21] A. Zhukovsky, J. Schultz, B. Smith, A. Radovinsky, D. Garnier, O. Filatov, *et al.*, “Charging Magnet for the Floating Coil of LDX”, *IEEE Trans. Appl. Supercond.*, **11** (2001) 1873.
- [22] A. Zhukovsky, P.C. Michael, J.H. Schultz, B.A. Smith, J.V. Minervini, J. Kesner, *et al.*, “First integrated test of the superconducting magnet system for the Levitated Dipole Experiment (LDX)”, *Fusion Eng. Des.* **75** (2005) 29.
- [23] A. Zhukovsky, D. T. Garnier, A. Radovinsky, “Thermal performance of the LDX floating coil”, Submitted to *Adv. in Cryo. Eng.*, 2005.
- [24] A. Zhukovsky and D.T. Garnier, “Operation of the Levitated Dipole Experiment Floating Coil”, Submitted to *IEEE Trans. Appl. Supercond.*, 2005.
- [25] P. C. Michael, A. Zhukovsky, B. A. Smith, J. H. Schultz, A. Radovinsky, J.V. Minervini, *et al.*, *IEEE Trans. Appl. Supercond.*, **13** (2003) 1620.
- [26] P. C. Michael, J. H. Schultz, B. A. Smith, P. H. Titus, A. Radovinsky, A. Zhukovsky, *et al.*, “Performance of the conduction-cooled LDX levitation coil”, *Adv. in Cryo. Eng.* **49** (2004) 701.
- [27] R. A. Dandl, A. C. England, W. B. Ard, H. O. Eason, M. C. Becker, and G. M. Hass, *Nuc. Fusion*, **4**,(1964) 344 .
- [28] H. P. Warren, M. E. Mauel, *Phys. Rev. Lett.*, **74** (1995) 1351; and H. P. Warren and M. E. Mauel, *Phys. Plasmas* **2**, (1995) 4185.
- [29] B. Levitt, D. Mastovsky, and M.E. Mauel, *Phys. Plasmas* **9**, (2002) 2507.
- [30] D. Maslovsky, B. Levitt, and M. E. Mauel, *Phys. Rev. Lett.* **90** (2003) 185001.